

CONJUGATE GRADIENT METHOD WITH ADJOINT PROBLEM APPLIED TO THE INVERSE DETERMINATION OF THE SPATIAL VARIATION OF THE BLOOD PERFUSION COEFFICIENT IN CANCEROUS TISSUES

LOPES C. F., karol.lopes@gmail.com

COLAÇO, M. J., colaco@asme.org

CALDEIRA, A. B., aldelio@ime.eb.br

SCOFANO NETO, F., scofano@ime.eb.br

Military Institute of Engineering

Dept. of Mechanical and Materials Engineering

Pç. Gen.Tibúrcio,80, Rio de Janeiro, RJ, 22290-270, Brazil

Abstract. *This work aims to establish an estimation of the blood perfusion coefficient in cancerous tissues by employing inverse strategies which make use of the Conjugate Gradient Method together with an Adjoint Problem. The physical problem was modeled by employing the Pennes' equation which consists of a standard heat diffusion equation together with an energy sink term that accounts for the blood flow within the biological tissue. Moreover, a source term is also present in this formulation which simulates the combined effect of the internal metabolic heat generation together with an external heat flux associated to the cancer treatment. In this work, the perfusion coefficient was considered to be related to the temperature field and spatially dependent. Accordingly, several different forms of the perfusion coefficients were simulated, all leading to good estimates. A study was also carried out in order to determine the adequate number of sensors which are needed to produce successful estimations. Simulated measurement with and without errors were taken into account yielding to good estimates of the perfusion coefficient.*

Keywords: *bioheat equation perfusion coefficient, inverse problem, parameter estimation.*

1. NOMENCLATURE

A	aspect ratio	T_{∞}	blood temperature within the vessel
Bi	Biot number	t	time
c	specific heat at constant pressure	x	horizontal coordinate
G	dimensionless heat generation	y	vertical coordinate
g	volumetric heat generation source	X	dimensionless horizontal coordinate
g_0	reference source of heating generation	Y	dimensionless vertical coordinate
h	heat transfer coefficient	w	modified perfusion coefficient
k	thermal conductivity	α	thermal diffusivity
L	tissue length	β	dimensionless eigenvalue
l	tissue thickness	ν	dimensionless eigenvalue
M	eigenfunction's norm	γ	dimensionless eigenvalue
N	eigenfunction's norm	θ	dimensionless temperature
P_f	dimensionless perfusion coefficient	ρ	density
T	tissue temperature	N.L.	noise level
T_0	initial temperature of the tissue		
T_a	arterial blood temperature		
T_p	skin surface temperature		

Subscripts

s	for the blood
t	for the tissue

2. INTRODUCTION

Cancer or malignant neoplasm is a disease characterized by the disorderly growth of a specific set of cells that multiply very fast, invading and damaging tissues or adjacent organs. Through a process called metastasis these cells spread out to various regions of the human body. The tumor is classified as malignant or benign depending on the anomalous cells properties that are responsible for its formation. If these cells show a fast and an uncontrolled growth, the tumor is said to be malignant. However, some benign tumors are capable to become malignant. (Cardoso, 2003).

The Cancer's treatment is typically implemented through a combination of the following techniques: surgery, chemotherapy, radiation, immunotherapy, together with drugs to treat side effects (Carmo *et al.*, 2005). The hyperthermia by radio frequency (microwave) is another commonly employed therapeutic technique used in treating cancer. It acts as a complementary therapy to the radiotherapy and chemotherapy, powering their efficiencies and further reducing the tumor. This medical procedure uses an external device that increases the temperature of the region being treated. The DNA of the cancer cells is altered when they are subjected to temperatures above 44°C. Thus, such malignant cells become inactive (Lima *et al.*, 2006).

A wide range of values for ideal temperature in the treatment of tumors by hyperthermia is found in the literature. Rawnsley *et al.* (1994) reported that the temperature of hyperthermal treatment for malignant tumors should not exceed 42.5 ° C. Giering *et al.* (1995) admit a thermal variation of 41.5 to 50 ° C. However, Rivolta *et al.* (1999) achieved partial or complete regression of tumors heating the tissue at temperatures between 41 and 43°C.

The main challenge associated with the success of treatment is to achieve a homogeneous distribution of temperature only within the region of the tumor, avoiding elevated temperatures at its surroundings. The blood perfusion coefficient is the major responsible for different values of temperature profiles in the malignant region (Lima *et al.*, 2006). Therefore, an accurate evaluation of this coefficient appears to be crucial for the outcome of the treatment.

The main contribution of this work is to estimate the perfusion coefficient in a thermal problem, modeled by the Pennes' equation. The Conjugate Gradient Method with Adjoint Problem for function estimation was used, where no *a priori* information about the function is needed. Simulated measurements, obtained through the solution of the Pennes' equation were used. As it shall be discussed in the following sections, good estimates were obtained for measurements with and without errors.

3. DIRECT PROBLEM

The physical problem considered here involves a two-dimensional and transient heat transfer process in a rectangular organic tissue. Initially, the entire region is supposed to be at a constant temperature T_0 . In the medical procedure, a heat flux is applied at the boundary of the affected tissue. In the mathematical model, this effect is taken into account by imposing an extra source term that adds to the usual metabolic heat. The outer surface of the tissue is supposed to be at a constant temperature T_p . In contrast, the innermost layer exchanges heat by convection with an adjacent blood vessel. Finally, the left and right walls are kept thermally insulated. The vascular contribution is simulated through the coefficient of perfusion. Although in the real case, the blood perfusion and metabolic heat effects are known to be temperature dependent, as a first approximation, both these terms are assumed to be only spatially dependent.

The mathematical equation that governs this physical problem was firstly developed by Pennes (1948). This equation in a dimensionless form, together with appropriate boundary and initial conditions, is present below.

$$\frac{\partial^2 \theta}{\partial X^2} + \frac{\partial^2 \theta}{\partial Y^2} - Pf \theta + G = \frac{\partial \theta}{\partial \tau} \quad 0 < Y < 1 \quad 0 < X < A \quad \tau > 0 \quad (1.a)$$

$$\frac{\partial \theta}{\partial X} = 0 \quad X = 0 \quad \tau > 0 \quad (1.b)$$

$$\frac{\partial \theta}{\partial X} = 0 \quad X = A \quad \tau > 0 \quad (1.c)$$

$$-\frac{\partial \theta}{\partial Y} + Bi \theta = Bi \theta_\infty \quad Y = 0 \quad \tau > 0 \quad (1.d)$$

$$\theta = 0 \quad Y = 1 \quad \tau > 0 \quad (1.e)$$

$$\theta = \theta_0 \quad 0 < Y < 1 \quad 0 < X < A \quad \tau = 0 \quad (1.f)$$

The Eqs.(2.a-h) define the parameters and the variables used in the proposed model.

$$\theta = \frac{T - T_a}{g_0 \frac{L^2}{k_t}}, G = \frac{g}{g_0}, A = \frac{l}{L}, X = \frac{x}{L}, Y = \frac{y}{L}, \tau = \frac{\alpha_t t}{L^2}, Pf = \frac{w_s c_s L^2}{k_t}, Bi = \frac{hL}{k_t} \quad (2.a-h)$$

An inspection on the left hand side of Eq. (1.a) reveals the presence of a sink and a source term. The sink term is the effect of convective capillary vascularization of the organic tissue, while the other represents the combined effects of metabolism and external irradiation.

The values adopted to each dimensionless parameter employed in this work ($Bi = 5$, $G = 1$, $\theta_0 = 0.003$ and $\theta_\infty = 0.001$) correspond to a tissue with a characteristic dimension of 3.0 cm, exposed to an external heat source of 50000 W/m³ and a rate of metabolic generation of 33800 W/m³ (Azevedo *et al.*, 2006). Also, the following parameters for blood were used: $\rho_s = 1060$ kg/m³ and $c_s = 3720$ J/ kg.K. The other parameters, were reported in Azevedo et al (2006).

4. INVERSE PROBLEM

In this work we estimated the spatially dependent perfusion coefficient (P_f), which appears as a heat source term in the Pennes' equation (1.a), using the Conjugate Gradient Method with Adjoint Problem for function estimation. In order to circumvent the lack of information due to the unknown P_f , some extra data is needed in order to solve this inverse problem. Such information is obtained through the measurement of temperature, by means of some sensors positioned either on the surface of inside the tissue being analyzed. In this work, the measured temperatures were obtained through a simulation of experiment, where the direct problem was solved using a known value of P_f , and the temperature field was used as an input data of the inverse problem. Some test cases involving random errors added to these temperatures were also analyzed and will be presented later.

The perfusion coefficients analyzed in this work were supposed to have spatial variation and, thus, we performed function estimation, where no information related to the functional form of P_f was assumed. In order to test the robustness of the method, five different forms for P_f were analyzed: constant, sinusoidal, triangular, square and step functions.

For the solution of the Inverse Problem, all the quantities of the mathematical model are assumed to be error free, except the perfusion coefficient P_f . Also, the random errors are taken to be Gaussian, with zero mean and known standard deviation.

The solution of the Inverse Problem considered in this paper involves the minimization of the following objective function:

$$S[P_f(x, y)] = \int_0^{\tau_f} \sum_{i=1}^M (\mu_i - \theta_i)^2 d\tau \quad (3.a)$$

where μ_i are the measured temperature by means of M sensors, θ_i is the estimated temperature, obtained iteratively through the solution of the direct problem with a estimate value of P_f and τ_f is the final time of the experiment.

The Conjugate Gradient Method with Adjoint Problem promotes the minimization of Eq. (3.a) through the following iterative process

$$P_f^{k+1}(x, y) = P_f^k(x, y) + \alpha^k d^k(x, y) \quad (3.b)$$

$$d^k(x, y) = -\nabla S[P_f^k(x, y)] + \gamma^k d^{k-1}(x, y) \quad (3.c)$$

$$\gamma^k = \frac{\int_0^{x_f} \int_0^{y_f} \{\nabla S[P_f^k(x, y)]\}^2 dy dx}{\int_0^{x_f} \int_0^{y_f} \{\nabla S[P_f^{k-1}(x, y)]\}^2 dy dx}, \quad k = 1, 2, 3.. \quad (3.d)$$

$$\gamma^k = 0, \quad k = 0$$

where k is the iteration counter, d is the direction of descent, α is the search step size and γ is the coefficient of conjugation, which was taken as the Fletcher Reeves equation in the present contribution. In order to minimize the functional given by Eq. (3.a) through the iterative process given by Eqs. (3.b-d), two auxiliary problems are needed and are discussed next: the sensitivity and the adjoint problem. The sensitivity problem is necessary in order to obtain the search step size value, appearing in Eq. (3.b), while the adjoint problem used to furnish the values of the gradient of the objective function (∇S), present in Eqs. (3.c,d). The search step size is derived by minimizing the objective function (3.a) with respect to α . It can be shown, after some manipulations, that the optimum search step size is given as:

$$\alpha^k = \frac{\int_0^{\tau_f} \sum_{i=1}^M [(\theta_i - \mu_i) \Delta \theta]^2 d\tau}{\int_0^{\tau_f} \sum_{i=1}^M (\Delta \theta_i)^2 d\tau} \quad (3.e)$$

The direct, sensitivity and adjoint problems were solved using the Finite Volume technique, where an implicit scheme was employed (Maliska, 2004). The computational code was validated by comparing the numerical solution of the direct problem with the one obtained by Azevedo *et al.* (2006) through the use of the Generalized Integral Transform Technique.

4.1 Sensitivity Problem

The sensitivity problem, whose solution gives the $\Delta\theta$ appearing on Eq. (3.e), is discussed in this section. In order to obtain such a problem, we consider that the temperature field is perturbed by a quantity $\Delta\theta$ as the perfusion coefficient is perturbed by a quantity ΔP_f . Thus, by replacing θ by $\theta + \Delta\theta$ and P_f by $P_f + \Delta P_f$ in the direct problem, given by Eqs. (1.a-f), and subtracting the result from the original equations, the following sensitivity problem is obtained:

$$\frac{\partial^2 \Delta\theta}{\partial X^2} + \frac{\partial^2 \Delta\theta}{\partial Y^2} - P_f \Delta\theta - \Delta P_f \theta = \frac{\partial \Delta\theta}{\partial \tau} \quad 0 < Y < 1 \quad 0 < X < 1 \quad \tau > 0 \quad (4.a)$$

$$\frac{\partial \Delta\theta}{\partial X} = 0 \quad X = 0 \quad \tau > 0 \quad (4.b)$$

$$\frac{\partial \Delta\theta}{\partial X} = 0 \quad X = 1 \quad \tau > 0 \quad (4.c)$$

$$-\frac{\partial \Delta\theta}{\partial Y} + Bi \Delta\theta = 0 \quad Y = 0 \quad \tau > 0 \quad (4.d)$$

$$\Delta\theta = 0 \quad Y = 1 \quad \tau > 0 \quad (4.e)$$

$$\Delta\theta = 0 \quad 0 < Y < 1 \quad 0 < X < 1 \quad \tau = 0 \quad (4.f)$$

It is worth noticing that the sensitivity and direct problem are coupled through the term $\Delta P_f \theta$, appearing on Eq. (4.a). Thus, the temperature field obtained during the solution of the direct problem must be stored for all grid points and all time steps for further use in the sensitivity problem. This causes the iterative process of the Conjugate Gradient Method to be computationally slow, due to the massive memory requirements.

4.2 Adjoint Problem

In this section, we discuss the adjoint problem, which is needed to obtain the gradient of the objective function, appearing on Eqs. (3.c,d). The adjoint problem is obtained by writing an extended function, also known as Lagrangean. This is needed because the minimization of the objective function, given by Eq. (3.a), must satisfy a constraint, which is given by the direct problem, Eq. (1.a). Thus, we multiply Eq. (1.a) by a Lagrange multiplier $\lambda(X, Y, \tau)$, integrate this result over the time and space and sum the result to the original objective function:

$$\bar{S}[P_f(x, y)] = \int_0^{\tau_f} \sum_{i=1}^M [\mu_i - \theta_i]^2 d\tau + \iiint_{\tau XY} \lambda \left[\frac{\partial^2 \theta}{\partial X^2} + \frac{\partial^2 \theta}{\partial Y^2} - P_f \theta + G - \frac{\partial \theta}{\partial \tau} \right] dYdXd\tau \quad (5.a)$$

$$\bar{S}[P_f(x, y)] = \iiint_{\tau xy} \lambda \left[\frac{\partial^2 \theta}{\partial X^2} + \frac{\partial^2 \theta}{\partial Y^2} - P_f \theta + G - \frac{\partial \theta}{\partial \tau} \right] + [\mu_i - \theta_i]^2 \delta_x(X - X_i) \delta_y(Y - Y_i) dYdXd\tau \quad (5.b)$$

Following the same procedure described for the sensitivity problem, we assume that the Lagrangean is perturbed by a quantity, when the perfusion coefficient P_f is perturbed by a quantity $P_f + \Delta P_f$.

$$\bar{S} + \Delta S = \iiint_{\tau XY} \left\{ \lambda \left[\frac{\partial^2 (\theta + \Delta\theta)}{\partial X^2} + \frac{\partial^2 (\theta + \Delta\theta)}{\partial Y^2} - (P_f + \Delta P_f) (\theta + \Delta\theta) + G - \frac{\partial (\theta + \Delta\theta)}{\partial \tau} \right] + [\mu_i - \theta_i]^2 \delta_x(X - X_i) \delta_y(Y - Y_i) \right\} dYdXd\tau \quad (5.c)$$

Thus, after some algebraic procedure, the following adjoint problem can be obtained

$$\frac{\partial^2 \lambda}{\partial X^2} + \frac{\partial^2 \lambda}{\partial Y^2} - \lambda P_f + 2[\theta_i - \mu_i] \delta_x(X - X_i) \delta_y(Y - Y_i) = -\frac{\partial \lambda}{\partial \tau^*} \quad 0 < Y < 1 \quad 0 < X < 1 \quad \tau^* > 0 \quad (6.a)$$

$$\frac{\partial \lambda}{\partial X} = 0 \quad X = 0 \quad \tau^* > 0 \quad (6.b)$$

$$\frac{\partial \lambda}{\partial X} = 0 \quad X = 1 \quad \tau^* > 0 \quad (6.c)$$

$$-\frac{\partial \lambda}{\partial Y} + Bi\lambda = 0 \quad Y = 0 \quad \tau^* > 0 \quad (6.d)$$

$$\lambda = 0 \quad Y = 1 \quad \tau^* > 0 \quad (6.e)$$

$$\lambda = 0 \quad 0 < Y < 1 \quad 0 < X < 1 \quad \tau^* = 0 \quad (6.f)$$

where τ^* is equal to $\tau^* = \tau_f - \tau$.

5 RESULTS AND DISCUSSION

In this section we present the results obtained for the estimate of the perfusion coefficient through the Conjugate Gradient Method with Adjoint Problem. As mentioned before, a constant P_f situation together with spatially dependent perfusion coefficients in the form of sinusoidal, triangular, square and step functions are employed as test cases in order to evaluate the robustness of the methodology discussed in this contribution.

Since we did not have access to real data, a simulation of experiment was conducted. Thus, the functional form of the perfusion coefficient was assumed known, and the direct problem was solved. The result was then considered as the measured temperatures, at the location of the sensors. In order to verify the stability of the method, we considered also measurements containing experimental errors, by adding a random error with Gaussian distribution and known standard deviation to the measured temperatures, obtained through the solution of the direct problem. In this paper we considered standard deviation equal to 1 and 5% of the local value of the temperature.

Two sets of test cases were analyzed: the first one involved one dimensional variations of the perfusion coefficient, while the second one dealt with two dimensional variation of P_f .

For the test cases where the perfusion coefficient depends only along the x coordinate, two test cases were analyzed: the first one considered 100 sensors with 0.3 mm of distance among them, and the second one considered 50 sensors with 0.6 mm of distance among them. The sensors were positioned at $Y = 0.9$, equivalent to 3 mm below the surface of the tissue. For both test cases, the frequency of measurement was taken as 0.01 Hz and the initial estimate for the Conjugate Gradient Method with Adjoint Problem was taken as 4.5. The total time of the experiment was taken as 2 h 43 min 37 s in all simulations and we considered an adipose tissue whose perfusion coefficient was taken as 5. The stopping criterion for the measurements with noise was based on the Principle of Discrepancy (Ozisik and Orlande, 2000). For the cases without measurement errors, the iterative process was interrupted with a tolerance of 10^{-11} .

Figures 1 to 5 present the results for this first test case. In these graphs, we present the estimate for the constant, sinusoidal, triangular, square and step functions.

Figure 1 shows the results for the constant function, where the exact value of the perfusion coefficient was taken as 5. It can be seen that both test cases (with 100 and 50 sensors) were able to recover the exact function for measurements without errors. When the experimental errors increased, with standard deviation equal to 1% of the local temperature, the estimate was slightly worst with the overall result similar for the cases with 100 and 50 sensors. In fact, looking at Table 1, one perceives that the RMS error for the cases with $\sigma=0.01\theta_{exact}$ was approximately the same for the case with 50 and 100 sensors (0.0210 and 0.0214, respectively). When the standard deviation was increased to 5% of the local temperature, both estimates deteriorate even more, with the case containing more sensors producing the worst estimate. A further investigation on Table 1 shows that the RSM error for $\sigma=0.05\theta_{exact}$ was equal to 0.0682, against 0.0279 for the test case with 50 sensors. However, as Fig. 1 suggests the maximum relative error between the exact and estimate values for the perfusion coefficient is less than 1.5%, which demonstrates the ability to recover such constant function by the Conjugate Gradient Method with Adjoint Problem.

Figure 2 shows the results for the sinusoidal variation of the perfusion coefficient along the x coordinate. Again the test cases with no experimental errors were able to fully recover the exact function, except for small deviations close to $X=0$. Similarly to the test case shown on Fig. 1, the objective function estimations was worst for the cases with $\sigma=0.05\theta_{exact}$ as one can verify from the large oscillations presented in Fig. 2. In fact, for $\sigma=0.05\theta_{exact}$, as previously discussed for the constant function, the RMS for the case with 100 sensors was greater than the test cases with 50 sensors (0.1398 against 0.0933 for 100 and 50 sensors, respectively), as one can verify from Table 1. For the case where the standard deviation was equal to 1% of the local temperature, both estimates (using 50 and 100 sensors) resulted in

similar accuracy, as one can verify from Fig. 2 and from the RMS errors shown on Table 1 (0.0596 and 0.0551 for 100 and 50 sensors, respectively).

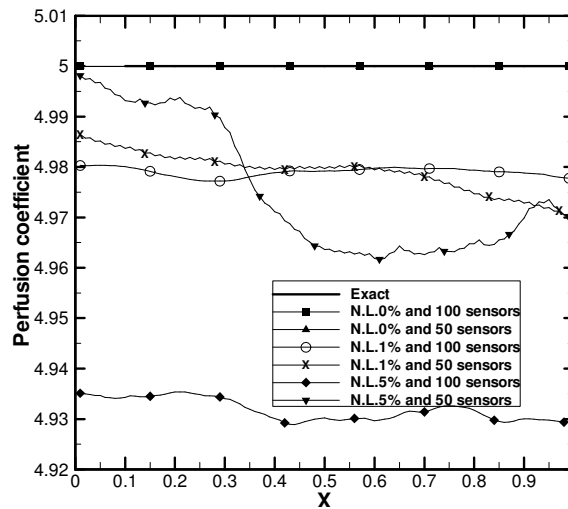


Fig. 1 Estimated perfusion as a constant function

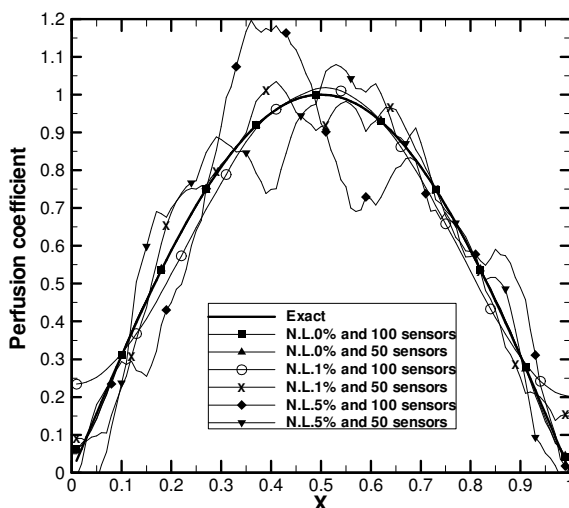


Fig. 2 Estimated perfusion as a sinusoidal function

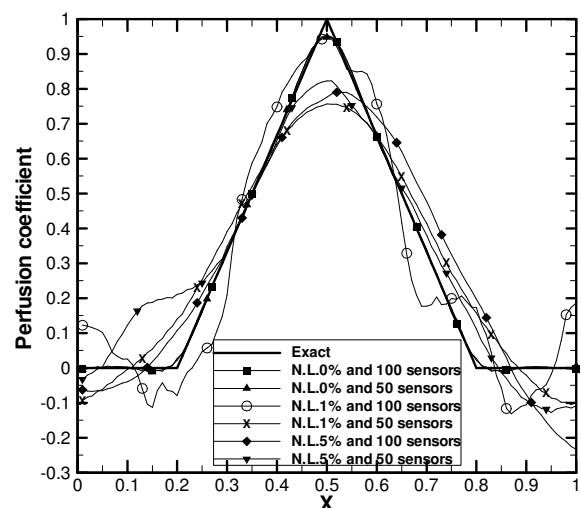


Fig. 3 Estimated perfusion as a triangular function

Figure 3 illustrates the evaluations when a triangular variation of the perfusion coefficient is considered. For this function, both test cases (with 50 and 100 sensors) were not able to fully recover the maximum value of the function. Also, they presented some discrepancies close to $X=0$. It is worth noticing that the RMS error presented in Table 1 for this particular function is, in fact, greater than the previous ones, for the test case with no measurement errors. For 100 sensors, the RMS error for $\sigma=0$ increased from 0.00005 for the constant function, to 0.0062 for the sinusoidal function and, finally for 0.0081 for the triangular function, indicating that such function is more difficult to be recovered, due to the discontinuity in the derivative close to the peak value. The same behavior is observed for the case with 50 sensors. The test case with 100 sensors and $\sigma=0.01\theta_{exact}$ was able to produce good results close to the peak value of the function, but presented large oscillations in the other regions. A similar behavior was observed for the test case with 50 sensors and $\sigma=0.05\theta_{exact}$.

From the analysis of Fig. 3, the test cases with the best performance for measurements with errors were the ones with 50 sensors and $\sigma=0.01\theta_{exact}$ and 100 sensors and $\sigma=0.05\theta_{exact}$, since they produced less oscillations. However, it is worth mentioning that neither of them was fully capable of recover the exact function, as one can verify from the analysis of Fig. 3 and Table 1, since all RMS errors for the cases with measurement errors presented very close numerical values.

Figure 4 shows the estimate of the perfusion coefficient with the form of a square function. Similarly to the triangular function, the best estimates were those without measurement errors. Also, since this function is even more difficult to be estimated, due to the discontinuities, the RMS errors are greater than the previous functions, as one can infer from Table 1. In fact, for 100 sensors without measurement errors, the RMS error increased from 0.0081 for the

triangular function, to 0.0827 for the square function. The same behavior is seen for the case with 50 sensors, where the RMS error was equal to 0.0092 for the triangular function and almost one order of magnitude greater (0.0953) for the square function. In order to verify the capability of the method to estimate discontinuous functions without any symmetry, the step function was also analyzed, and it is shown in Fig. 5. Here, once again, the measurements without experimental errors were capable of estimate with relatively good accuracy, the exact function. It is interesting to note that, since the step function has only one discontinuity, the RMS errors associated with its estimate are lower than the ones related to the square functions, although they are still greater than the ones associated with the triangular function, as one can verify from Table 1. For the cases with measurement errors, the ones with 50 sensors and $\sigma=0.01 \theta_{exact}$, as well as, 100 sensors and $\sigma=0.01 \theta_{exact}$ presented the best estimates for the step function.

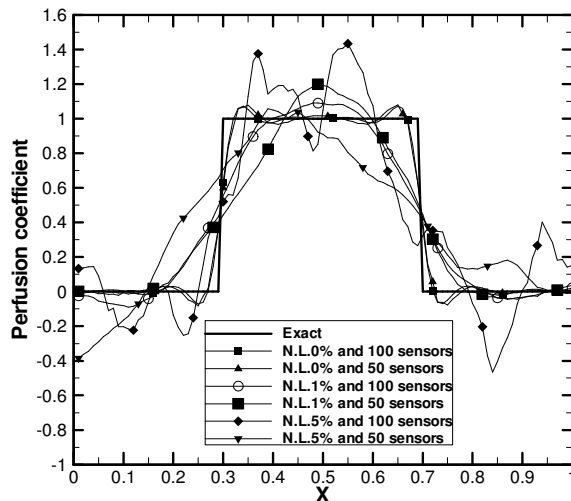


Fig. 4 Estimated perfusion as a square function

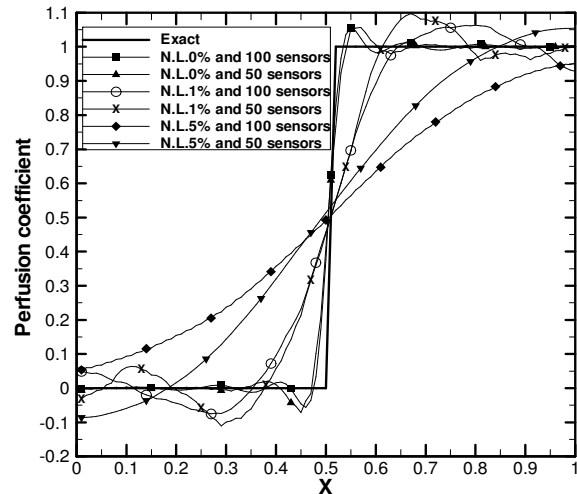


Fig. 5 Estimated perfusion as a step function

TAB. 1 Estimated blood perfusion with 100 and 50 sensors
 Grid 100x100, $G = 2.48 \text{ e Tol.} = 10^{-11}$

Functions	Standard deviation	Initial guess equal to 4.5 and sensors located at $Y = 0.9$			
		100 sensors		50 sensors	
		RMS Error	Objective function	RMS Error	Objective function
Constant	$\sigma = 0$	0.00005	9.2908×10^{-12}	0.00007	9.4679×10^{-12}
	$\sigma = 0.01 \theta_{exact}$	0.0214	6.7621×10^{-5}	0.0210	3.4126×10^{-5}
	$\sigma = 0.05 \theta_{exact}$	0.0682	8.0704×10^{-3}	0.0279	1.6546×10^{-3}
Sinusoidal	$\sigma = 0$	0.0062	9.9840×10^{-12}	0.0079	9.9740×10^{-12}
	$\sigma = 0.01 \theta_{exact}$	0.0596	1.3471×10^{-4}	0.0551	6.8568×10^{-5}
	$\sigma = 0.05 \theta_{exact}$	0.1398	3.4147×10^{-3}	0.0933	1.6857×10^{-3}
Triangular	$\sigma = 0$	0.0081	9.9918×10^{-12}	0.0092	9.9801×10^{-12}
	$\sigma = 0.01 \theta_{exact}$	0.0946	1.4205×10^{-4}	0.0905	7.3789×10^{-5}
	$\sigma = 0.05 \theta_{exact}$	0.1083	3.6799×10^{-3}	0.0942	1.8897×10^{-3}
Square	$\sigma = 0$	0.0827	1.0142×10^{-10}	0.0895	9.7157×10^{-11}
	$\sigma = 0.01 \theta_{exact}$	0.1782	1.4984×10^{-4}	0.0953	7.6936×10^{-5}
	$\sigma = 0.05 \theta_{exact}$	0.2792	3.8992×10^{-3}	0.0996	1.9986×10^{-3}
Step	$\sigma = 0$	0.0602	7.4910×10^{-11}	0.0680	7.0648×10^{-11}
	$\sigma = 0.01 \theta_{exact}$	0.1422	1.4097×10^{-4}	0.1393	7.5861×10^{-5}
	$\sigma = 0.05 \theta_{exact}$	0.2574	3.7724×10^{-3}	0.2159	1.9759×10^{-3}

The next results present the estimate of the perfusion coefficient with a two dimensional variation. In all these test cases, we used a grid with 10000 volumes. The initial guess for the Conjugate Gradient Method with Adjoint Problem was set equal to 0.1 for all subsequent test cases. In these test cases, we used two different configurations. Initially, the sensors were introduced in all the grid points in order to verify the capability of the method with the maximum of information possible to be obtained from the problem. Then, we used only 100 sensors, located 3 mm below the surface

located at $Y=1$. In both test cases, the distance among the sensors was equal to 0.3 mm. The iterative process stopped either when the value of the objective function was equal to 10^{-11} or when the iterative process reached 2000 iterations.

Figure 6 shows the exact function and Fig. 7 illustrates the estimated one, using sensors in all grid points, where the function was relatively well captured. However, for the case where only 100 sensors located 3 mm below the $Y=1$ surface did not present very good results, as one can verify from the results presented at Fig. 8. Such poor estimates are due to the lack of information related to the bi-dimensional variation of the perfusion coefficient. Thus, it is not possible to use sensors only close to the boundary and more intrusive sensors are needed. However, it is worth noticing that the estimated perfusion suggested that a non-uniform P_f was present in a vicinity of the discontinuity, although it was not able to capture it. Table 2 shows the RMS errors related to this estimate, where one can verify that the large values are for the case with only superficial sensors.

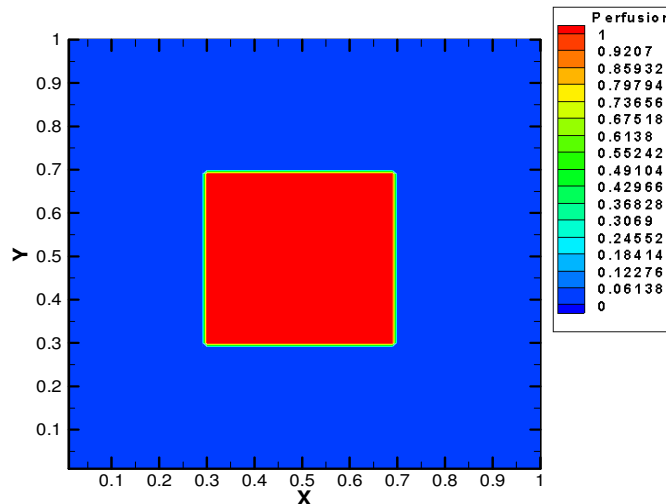


Fig.6 Exact function

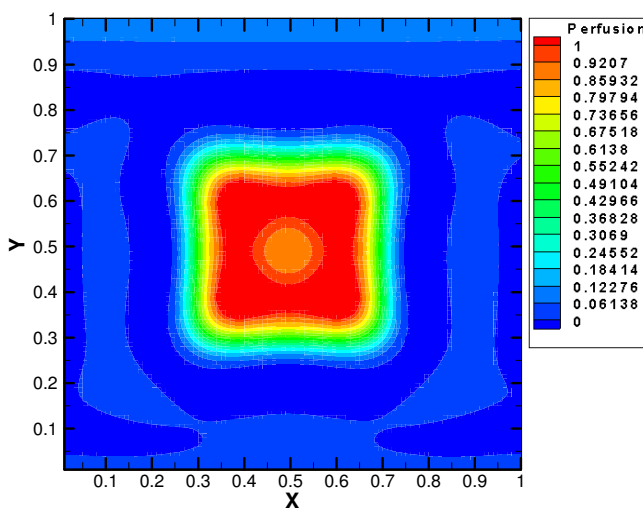


Fig.7 Estimated perfusion with sensors in all points

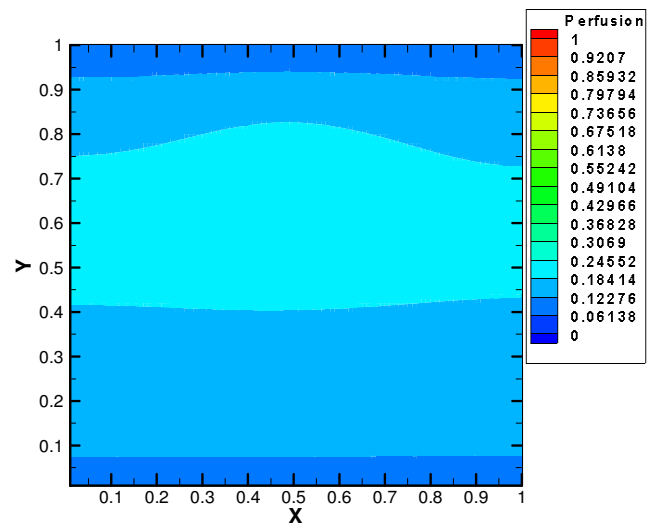


Fig.8 Estimated perfusion with sensors at $Y=0.9$

In order to verify the stability of the method, the same test cases presented in Figs. 7 and 8 are repeated, but with measurement errors. In this case, the standard deviation was set equal to 1% of local temperature value. Figures 9 and 10 depict such situations where one can verify that the estimate yields poor results due to the presence of the errors. However, the estimated value of the perfusion coefficient is not too different from those obtained for measurements without errors. In fact, looking at Table 2, one can verify that the RMS errors are close to one another, corroborating such observation.

Finally, we tried to recover two discontinuities, having different peak values, as shown in Fig. 11. Fig. 12 shows the results using measurements without errors, for sensors located in all grid points. It can be seen that the estimate is very good, for this extremely complex test case.

Fig. 13 shows the results obtained with the use of 199 sensors. In this test case, 100 sensors were located 3 mm below the $Y=1$ surface and 99 sensors are positioned at $X=0.5$, for different depths. The results show that it is possible to evaluate approximately the location of the tumors, although their peak values are not properly captured. Figure 14

studies the same situation, but without the 99 extra sensors, where it can be seen that the estimate is very poor, thus confirming the needed of inserting more sensors inside the domain.

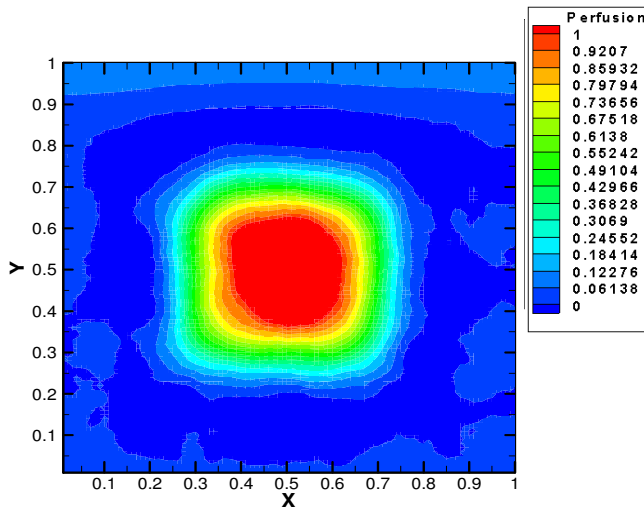


Fig.9 Estimated perfusion with sensors in all points and $\sigma=0.01\theta_{exact}$

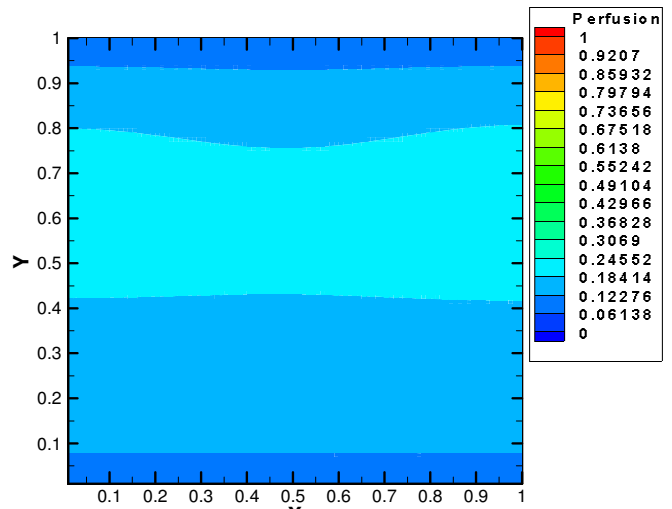


Fig.10 Estimated perfusion with sensors at $Y=0.9$ and $\sigma=0.01\theta_{exact}$

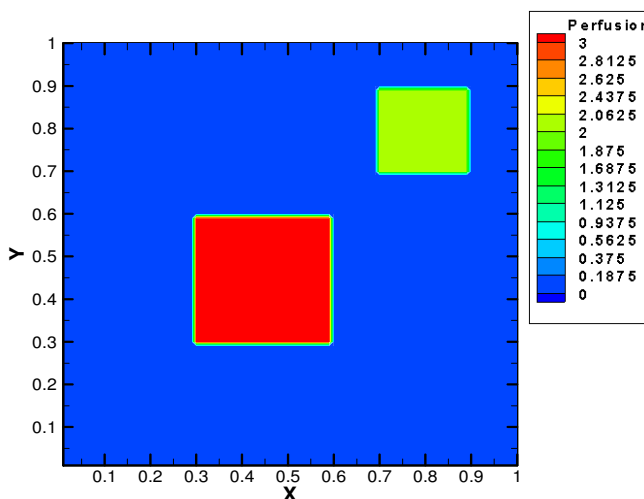


FIG. 11 Exact function

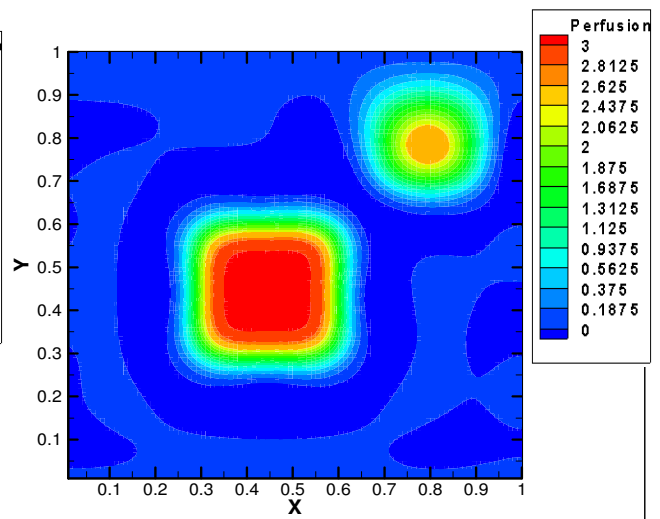


Fig.12 Estimated perfusion with sensors in all points

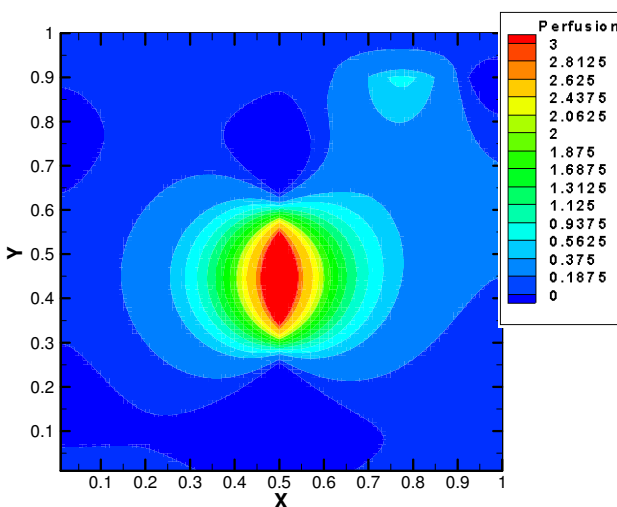


Fig.13 Estimated perfusion with 199 sensors

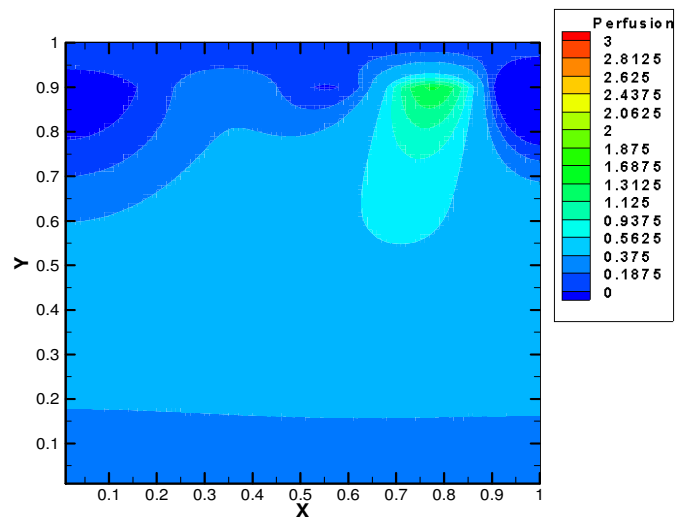


Fig.14 Estimated perfusion with 100 sensors

TAB. 2 Estimation of blood perfusion to form two-dimensional of sensors for various

	Standard deviation	Sensors	RMS Error
Square function (2 tumors)	$\sigma = 0$	10000	0.4235
		199	0.6141
		100	0.8658
		10000	0.1125
		100	0.3572
	$\sigma = 0.01 \theta_{exact}$	10000	0.1606
		100	0.4195

6. CONCLUSIONS

The research conducted in this involved the identification of the blood perfusion in a tissue with a tumor, subjected to a treatment by hyperthermia, aiming to improve the quality of treatment in non-operable tumors.

From the estimates of the blood perfusion conducted in this work, it is clear that the Conjugate Gradient Method was capable to recover functions with discontinuities, as well as functions with measurement errors up to 1% of the local value of the temperature, for one-dimensional variations of the perfusion coefficient, when the sensors were located close to the surface of the tissue.

For functions with two dimensional variations, more sensors were needed in order capture the discontinuities of the function.

Further studies are needed for test cases where the physical properties have temperature dependence. Also, the three dimensional case should be studied.

7. ACKNOWLEDGEMENTS

This work was partially funded with resources from FAPERJ, CAPES and CNPq, brazilian agencies for scientific and technological development.

8. REFERENCES

- Azevedo, M. D. B., Guedes, R. O. and Scofano Neto, F., 2006 "Analytical solution to the two dimensional transient bioheat equation with convective boundary conditions", Proceedings of the 11th Brazilian Congress of Thermal Sciences and Engineering – ENCIT.
- Cardoso, I.C.R.A., 2003, "Avaliações da radioterapia de megavoltagem, braquiterapia por implantes de sementes de Iodo-125 e/ ou associações, através de monitoração de parâmetros preditivos e de antígeno prostático específico (PSA) de pacientes portadores de câncer de próstata". Dissertação (Mestrado em Ciências e Técnica Nucleares) - Escola de Engenharia da UFMG, Belo Horizonte.
- Carmo, E.J.S., Fonseca, C.A. and Rodriguez, A.J.L., 2005, "Atualizações em câncer: Tratamento", in: III Seminário de Iniciação Científica e I Jornada de Pesquisa e Pós-Graduação da UEG - Anápolis, GO.
- Giering, K., Lamprecht, I., Minet, O. and Handke, A., 1995, "Determination of specific heat capacity of healthy and tumorous human tissue". *Thermochimica Acta*, Vol.251, pp. 199-205.
- Lima, R.C.F., Lyra, P.R.M. and Guimarães, C.S.C., 2006, "Modelagem computacional da biotransferência de calor no tratamento por hipertermia em tumores de duodeno através do método de volumes finitos em malhas não estruturadas", *Revista Brasileira de Engenharia Biomédica*, Vol. 22, pp. 119-129.
- Maliska, C. R., 2004, "Transferência de calor e mecânica dos fluídos computacional", LTC- Livros Técnicos e Científicos, Editora S.A, Rio de Janeiro, RJ.
- Ozisik, M. N. and Orlande, H. R. B., 2000, "Inverse heat transfer: fundamentals and applications", Taylor & Francis, New York, NY.
- Pennes, H.H., 1948, "Analysis of Tissue and Arterial Blood Temperatures in the Resting Human Forearm", *Journal of Applied Physiology*, pp. 93-122.
- Rawnsley, R.J., Roemer, R.B. and Dutton, A.W., 1994, "The simulation of discrete vessel in experimental hyperthermia", *Journal of Biomechanical Engineering*, pp. 256-262.
- Rivolta, B., Inzoli, F., Mantero, S. and Severine, S., 1999, "Evaluation of temperature distribution during hyperthermic treatment in biliary tumors: a computational approach", *Journal of Biomechanical Engineering*, pp. 141-147.

9. RESPONSIBILITY NOTICE

The authors are the only responsible for the printed material included in this paper.